Electrochemical Assembling/Disassembling of Helicates with Hysteresis

Valeria Amendola,[†] Luigi Fabbrizzi,*[,†] Luca Gianelli,[‡] Cristina Maggi,[†] Carlo Mangano,[†] Piersandro Pallavicini,[†] and Michele Zema[‡]

Dipartimento di Chimica Generale, Università di Pavia, via Taramelli 12, I-27100 Pavia, Italy, and Centro Grandi Strumenti, Università di Pavia, via Bassi 21, I-27100 Pavia, Italy

Received October 18, 2000

A series of eight tetradentate, ditopic, bisimino bisheterocyclic ligands (**1**−**8**), and their complexes with Cu^{I} and Cu^{II}, have been studied in CH_3CN solution, by means of ^1H NMR, mass, and UV/vis spectroscopy, while the crystal and molecular structure of the Cu^{II} complexes $[Cu(\mathbf{3})](CF_3SO_3)_2$ and $[Cu(\mathbf{4})](CF_3SO_3)_2$ and of the Cu^{I} complexes $[Cu_2(\mathbf{4})_2](ClO_4)_2$ and $[Cu_2(\mathbf{5})_2](ClO_4)_2$ have been determined by X-ray diffraction methods. The Cu^{II} complexes are monomeric, almost square-planar structures, both in solution and in the solid state, while the Cu^{I} complexes are two-metal, two-ligand dimers which can be both helical and "box-like" in the solid, while they adopt a simple helical configuration in acetonitrile solution. The systems made of ligands **1**−**8** and copper are bistable, as under the same conditions either the Cu^{I} helical dimers or the Cu^{II} monomers can be obtained and are stable. The electrochemical behavior of the 16 copper complexes has been studied in acetonitrile solutions by cyclic voltammetry. One reduction and one oxidation wave were found in all cases, which display no return wave and are separated by a 500−1000 mV interval. Irreversibility is due to the fast self-assembling process that follows the reduction of $[Cu^{II}(\mathbf{L})]^{2+}$ and to the fast disassembling process that follows the oxidation of $[Cu^{I}_2(\mathbf{L})_2]^{2+}$ ($\mathbf{L}$ = **1**−**8**). However, the overall [oxidation+disassembling] or [reduction+self-assembling] processes, i.e., $[Cu^{I}_2(\mathbf{L})_2]^{2+} = 2[Cu^{II}(\mathbf{L})]^{2+} + 2e^-$, are fully reversible. Moreover, CV profiles show that solutions containing copper and **L** undergo hysteresis on changing the applied electrochemical potential: in the same potential interval, the systems can exist in solution as either $[Cu^{I}_2(\mathbf{L})_2]^{2+}$ or $[Cu^{II}(\mathbf{L})]^{2+}$, depending on the electrochemical history of the solution. Moreover, by changing the structural or donor features of the ligands it is possible to modulate the potentials at which the system undergoes a transition from one to the other of its two possible states, in the hysteresis cycle. In addition, the spectral properties of the Cu^{I} and Cu^{II} complexes of the considered ligands make these systems good candidates for storing information in solution, which can be electrochemically written or erased and spectroscopically read.

Introduction

Recent developments in the area of (supra)molecular machines and devices have led to molecules that behave as logical operators in solution.[1] Although in a very futuristic perspective, they could provide an alternative to the well-established solid-state silicon-based technology, leading to the construction of chemical computers, whose components work in a "wet" environment.[2] Along this view, interest should focus also on suitable "molecular memories"[3] for the wet chemical computer. Thus can be considered those (supra)molecular systems capable of storing one information per (supra)molecule and for which the information writing, reading, and erasing processes can be carried out in solution. As a general requirement, a substance capable of "memorizing" an information must be bistable and should display hysteresis.[4] This requires that (i) the chosen substance must be able to exist in two different states (S_1 and S_2), which change one into the other on variation of the value of an external parameter (P); (ii) there must exist a range of values of P in which the substance can be found in state S_1 or S_2, depending on the "history" of the system, as it is schematized in Figure 1a. Moreover, provided that the chosen substance has different properties in its two states (e.g., S_1 is colorless, while S_2 is strongly absorbing), an information can be stored in a "portion" of it by changing P to P_1 and switching from S_1 to S_2

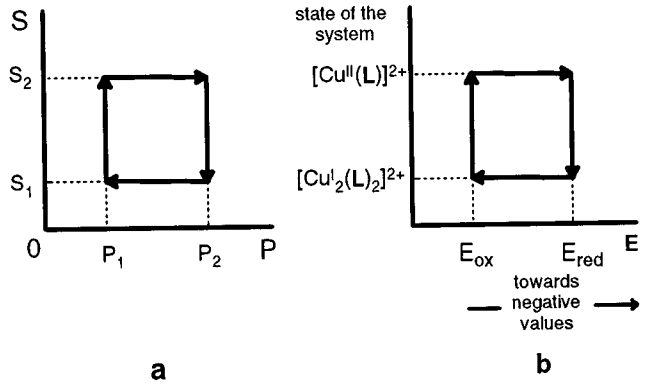

Figure 1. (a) Scheme for a hysteresis cycle. (b) Schematization of the electrochemical transformation of $[Cu^{I}_2(\mathbf{L})_2]^{2+}$ into $[Cu^{II}(\mathbf{L})]^{2+}$, and vice versa, as a hysteresis cycle ($\mathbf{L}$ = **1**−**8**). The *E*-axis values decrease toward the right, to conform to the E-axis orientation of a typical CV experiment.

* Corresponding author. E-mail: fabbrizz@unipv.it.
† Dipartimento di Chimica Generale.
‡ Centro Grandi Strumenti.

(1) (a) De Silva, A. P.; Gunaratne, H. Q. N.; McCOy, C. P. *Nature* **1993**, *364*, 42. (b) De Silva, A. P.; McClenaghan, N. D. *J. Am. Chem. Soc.* **2000**, *122*, 3965. (c) Credi, A.; Balzani, V.; Langford, S. J.; Stoddart, J. F. *J. Am. Chem. Soc.* **1997**, *119*, 2679. (d) Pina, F.; Maestri, M.; Balzani, V. *Chem. Commun.* **1998**, 245.
(2) Bradley D. *Science* **1993**, *259*, 890.
(3) Tomita A.; Sano M. *Inorg. Chem.* **2000**, *39*, 200.
(4) (a) Bolvin, H.; Khan, O.; Vekhter, B. *New. J. Chem.* **1991**, *15*, 889. (b) Kahn, O.; Launay, J. P. *Chemtronics* **1988**, *3*, 140.

10.1021/ic001155a CCC: $20.00
Published on Web 06/08/2001

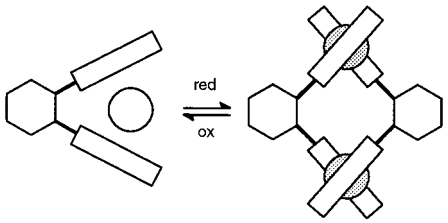

Figure 2. Pictorial sketch of the redox-driven self-assembling/disassembling process for Cu^{I} helicates/Cu^{II} square-planar complexes.

(writing process, colored portion in the example). The information (state S_2, color) is mantained unless P is not made to vary back to P_2, when the substance is switched again to S_1 (erasing process, colorless substance). The "reading" of the stored information can be done, in this example, by spectroscopy: when the chosen portion of substance absorbs light, a "bit value" of 1 is read through it, while the colorless substance corresponds to a "bit value" of 0. A lot of interest has been placed on reducing the portion of substance displaying hysteresis to a single molecule. Hysteresis for molecular systems has been described in several papers, although in most cases it concerned solid-state interacting or noninteracting molecules.[5] A few examples of molecular hysteresis in solution have also been reported, in which the external parameter made to change is the applied redox potential.[6] In the latter cases, changing the applied potential up to a certain value (E_{ox}) makes the system oxidize *and* rearrange to a different isomeric form: reduction of the oxidized and isomerized molecule then takes place at a potential (E_{red}) that is distinctly lower than E_{ox} and is followed by a back-isomerization that leads again to the starting species. In the $E_{ox}-E_{red}$ interval the system can thus exist in two different forms, depending on its electrochemical hystory. A comparable behavior is found for a small number of supramolecular systems, consisting of tetradentate ditopic ligands with sp^2 nitrogen donors and copper cations:[7] when copper is in oxidation state II, monomeric, almost square-planar 1:1 complexes are formed, but when they are electrochemically reduced to Cu(I) (at E_{red} potential), a spontaneous self-assembling process takes place to form helical 2:2 complexes. Making the applied redox potential vary back toward positive values, oxidation and disassembling are obtained at E_{ox}, to restore the original monomeric Cu(II) species. The overall process is sketched in Figure 2. The separation between E_{ox} and E_{red} has a value of some hundreds of mV, and in the $E_{ox}-E_{red}$ interval the system can be found either in a monomeric Cu(II) or in a helical, dimeric Cu(I) form, depending on the electrochemical history of the solution. Interestingly, the assembling/disassembling processes taking place after the electrochemical events are very fast for some of these systems, and dramatic changes in color are observed:[7] Cu(II) complexes display weak d−d bands (ϵ = 50−250) in the visible region, while Cu(I) complexes display strong MLCT bands (ϵ = 3000−15000) in the same region. According to this, they can be proposed as candidates for the storage of information in solution. In this work, a set of systems capable of fast electrochemical Cu(I) helical dimer/Cu(II) monomer assembling/disassembling processes with hysteresis is presented, based on tetradentate ditopic ligands featuring two imines and two nitrogen heterocycles, subdvivided into two bidentate imino-heterocycle halves. A set of rigid and elastic fragments separating the two imino-heterocycle halves of the ligands has been used and combined with a set of different nitrogen heterocycles to give ligands **1**−**8**. The solid-state and solution structure of their Cu(I) (dimeric, helical) and Cu(II) (monomeric) complexes have been ascertained by X-ray diffraction and UV/vis, ^{1}H NMR, and mass (ESI) spectrometry. It has been shown that, in the copper complexes, the oxidation and reduction potentials and the width of the interval between them, together with the position of the MLCT Cu(I) band, are tuned by the nature of the spacer and of the binding heterocycle. Moreover, the rate and reversibility of the Cu(II)/Cu(I) changes, i.e., of the assembling/dissassembling processes, have been checked by cyclic voltammetry and controlled potential coulometry experiments.

Experimental Section

Synthesis of the Ligands. The syntheses of compounds **1** and **7** have been already described.[7b,8] In this work, ligands **2**−**6** and **8** have been prepared by reaction of a diamine with the pertinent dialdehyde, following a general procedure that is slightly different from the methods published for **1** and **7**. All the employed diamines (ethylenediamine for compound **8**; racemic *trans*-1,2-diaminocyclohexane for compounds **2**-**4**; *cis*-1,2-diaminocyclohexane for compounds **5** and **6**) and all the aldehydes (2-quinolinecarboxaldehyde for compounds **5** and **8**; 2-thiazolecarboxaldehyde for compound **3**; 6-methyl-2-pyridinecarboxaldheyde for compound **4**) are commercially available and were used as purchased, except 6-phenanthridinecarboxaldehyde (parent compound for ligands **2** and **6**), which has been prepared as described in the literature.[9] In a typical ligand synthesis, 1.5 mmol of diamine were dissolved in 20 mL of CH_2Cl_2 and treated with 3.0 mmol of aldehyde, and the obtained solution was stirred at room temperature for 24 h. An excess of anhydrous $MgSO_4$ was then added, to remove the water produced by the imine formation, and the obtained mixture was further stirred at room temperature for 2 h and filtered. The solvent was then removed on a rotary evaporator to give a waxy material, which on treatment with 10 mL of *n*-hexane quickly transformed into a microcrystalline substance. Filtration, washing with further *n*-hexane (2 × 5 mL), and drying under vacuum yielded the desired pure product, which was characterized by C, H, N analysis and NMR and IR spectroscopy. Yields and characterization data are reported in Table S1 for ligands **2** (*N*,*N*′-bis(phenanthridin-6-ylmethylene)cyclohexane-*trans*-1,2-diamine), **3** (*N*,*N*′-bis(thiazol-2-ylmethylene)cyclohexane-*trans*-1,2-diamine), **4** (*N*,*N*′-bis(6-methyl-pyridin-2-ylmethylene)-cyclohexane-*trans*-1,2-diamine), **5** (*N*,*N*′-bis(quinolin-2-ylmethylene)-cyclohexane-*cis*-1,2-diamine), **6** (*N*,*N*′-bis(phenanthridin-6-ylmethylene)cyclohexane-*cis*-1,2-diamine), and **8** (*N*,*N*′-bis(quinolin-2-ylmethylene)ethane-1,2-diamine).

Synthesis of the Metal Complexes. The synthesis of complexes $[Cu^{I}_2(\mathbf{1})_2](ClO_4)_2$ and $[Cu^{II}(\mathbf{1})](CF_3SO_3)_2$ have already been described.[7b] In this work, complexes $[Cu^{I}_2(\mathbf{L})_2](ClO_4)_2$ (**L** = **2**−**8**) and $[Cu^{II}(\mathbf{L})](CF_3SO_3)_2$ (**L** = **3**−**8**) have been prepared according to a common, straightforward procedure, i.e., by mixing 0.1 mmol of the chosen ligand with the same molar amount of $[Cu(CH_3CN)_4]ClO_4$ or $Cu(CF_3SO_3)_2$ in 5 mL of CH_3CN, in air and at room temperature. Precipitation of

(5) (a) Sarkar, S.; Satchell, J. S. *Europhysics Lett.* **1987**, *3*, 797. (b) Ben-Aryeh, Y.; Bowden, C. M.; Englund, J. C. *Phys. Rev., A* **1986**, *34*, 3917.

(6) (a) Connelly, N. G.; Raven, S. J.; Carriedo, G. A.; Riera, V. *J. Chem. Soc., Chem. Commun.* **1986**, 992. (b) Vallat, A.; Person, M.; Roullier, L.; Laviron, E. *Inorg. Chem.* **1987**, *26*, 332. (c) Sano, M.; Taube, H. *J. Am. Chem. Soc.* **1991**, *113*, 2327.

(7) (a) Gisselbrecht, J.-P.; Gross, M.; Lehn, J.-M.; Sauvage, J.-P.; Ziessel, R.; Piccinni-Leopardi, C.; Arrieta, J. M.; Germain, G.; Van Meerssche, M. *Nouv. J. Chim.* **1984**, *8*, 661. (b) Amendola, V.; Fabbrizzi, L.; Linati, L.; Mangano, C.; Pallavicini, P.; Pedrazzini, V.; Zema, M. *Chem. Eur. J.* **1999**, *5*, 3679. (c) Yao, Y.; Perkovic, M. W.; Rillema, D. P.; Woods, C. *Inorg. Chem.* **1992**, *31*, 3956. (d) Potts, K. T., Keshavarz-K, M.; Tham, F. S.; Abruña, H. D.; Arana, C. R. *Inorg. Chem.* **1993**, *32*, 4422. (e) Potts, K. T.; Keshavarz-K, M.; Tham., F. S.; Abruña, H. D.; Arana, C. *Inorg. Chem.* **1993**, *32*, 4450. (f) Ziessel, R.; Harriman, A.; Suffert, J.; Youinou, M. T.; De Cian, A.; Fischer, J. *Angew. Chem., Int. Ed. Engl.* **1997**, *36*, 2509 (see also, for related discussion: El-ghayouy, A.; Harriman, A.; De Cian, A.; Fischer, J.; Ziessel, R. *J. Am. Chem. Soc.* **1998**, *120*, 9973).

(8) Busch, D. H.; Bailar, J. C., Jr. *J. Am. Chem. Soc.* **1956**, *78*, 1137.

(9) Eicher, T.; Kruse, A. *Synthesis* **1985**, 612.

the pure, crystalline product was then obtained by slow diffusion of diethyl ether in the acetonitrile solution. Only $[Cu^{II}(\mathbf{2})](CF_3SO_3)_2$ had

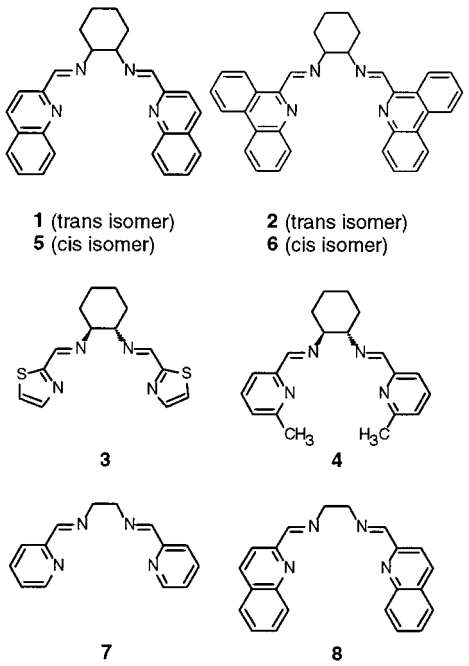

to be synthesized in a different way, due to the slow spontaneous reduction to the Cu^{I} complex observed in acetonitrile. In this case 30 mg (0.06 mmol) of ligand **2** were dissolved in 50 mL dichloromethane and treated with 21.7 mg (0.06 mmol) of $Cu(CF_3SO_3)_2$. The mixture was then efficiently stirred at room temperature, until all the copper salt had reacted with **2** and consequently dissolved. The solvent was then removed on a rotary evaporator to give the solid complex, which was collected and washed with 1 mL of CH_3CN and 5 mL of diethyl ether. All the obtained products were characterized by C, H, N analysis and NMR (Cu(I) complexes), IR, and mass (ESI) spectra. In particular, the latter technique, performed on acetonitrile solutions of the obtained solids, revealed $[Cu^{II}(\mathbf{L})CF_3SO_3]^+$ species and $[Cu^{I}_2(\mathbf{L})_2ClO_4]^+$ species. Yields and characterization data are collected in the Supporting Information as Table S2 (Cu(II) complexes) and Table S3 (Cu(I) complexes). The obtained Cu(II) complexes are $[Cu^{II}(\mathbf{2})](CF_3SO_3)_2$, $[Cu^{II}(\mathbf{3})](CF_3SO_3)_2$, $[Cu^{II}(\mathbf{4})](CF_3SO_3)_2$, $[Cu^{II}(\mathbf{5})](CF_3SO_3)_2$, $[Cu^{II}(\mathbf{6})](CF_3SO_3)_2$, $[Cu^{II}(\mathbf{7})](CF_3SO_3)_2$, and $[Cu^{II}(\mathbf{8})](CF_3SO_3)_2$, while the obtained Cu(I) complexes are $[Cu^{I}_2(\mathbf{2})_2](ClO_4)_2 \cdot 2CH_3CN$, $[Cu^{I}_2(\mathbf{3})_2](ClO_4)_2$, $[Cu^{I}_2(\mathbf{4})_2](ClO_4)_2$, $[Cu^{I}_2(\mathbf{5})_2](ClO_4)_2$, $[Cu^{I}_2(\mathbf{6})_2](ClO_4)_2 \cdot 2CH_3CN \cdot H_2O$, $[Cu^{I}_2(\mathbf{7})_2](ClO_4)_2 \cdot 2CH_3CN$, and $[Cu^{I}_2(\mathbf{8})_2](ClO_4)_2$.

Physical Measurements. UV/vis spectra were recorded on a Hewlett-Packard 8453 diode array spectrophotometer, mass spectra (ESI) on a Finnigan MAT TSQ 700 instrument, NMR spectra on a Bruker AMX 400 spectrometer, and IR spectra on a Mattson 5000 FT-IR instrument.

Spectrophotometric Titrations. Titrations were performed on 30−50 mL samples (kept under a dinitrogen stream) of 10^{-3}−10^{-4} mol L^{-1} solutions of ligand in CH_3CN, by microadditions of a CH_3CN solution of either $[Cu^{I}(CH_3CN)_4]ClO_4$ or $Cu(CF_3SO_3)_2$. In a typical experiment, a 1:1 metal/ligand molar ratio was reached after addition of 20 portions of 10 μL each of the metal salts solutions.

Electrochemistry and Spectroelectrochemistry. The apparatus for coupled controlled potential coulometry−UV/vis spectral measurements was assembled as already described.[7b] Cyclic voltammetry studies were carried out in anhydrous CH_3CN solution, made 0.1 mol L^{-1} in $(t\text{-Bu})_4NClO_4$. The working electrode was a platinum microsphere and the counter electrode a platinum wire. A SCE electrode was used as the reference, dipped in the working solution through a jacket filled with 0.1 M aqueous $NaClO_4$. The measured potential values were also checked by using a platinum wire as the reference electrode and by adding ferrocene to the working solution as an internal standard (the potential values referred to the Fc^+/Fc couple can be transformed into values referred to SCE, or vice versa, considering an $E_{1/2}$ value of 425 mV vs SCE, in CH_3CN, determined for the Fc^+/Fc couple[10]).

Table 1. Crystal and Refinement Data for Cu(I) Complexes

	$[Cu^{I}_2(\mathbf{5})](ClO_4)_2 \cdot 2CH_3CN$	$[Cu^{I}_2(\mathbf{4})](ClO_4)_2$
formula	$C_{56}H_{54}Cl_2Cu_2N_{10}O_8$	$C_{40}H_{48}Cl_2Cu_2N_8O_8$
molecular weight	1193.07	966.84
cryst color	black	brown
cryst size (mm)	0.56 × 0.70 × 0.98	0.07 × 0.07 × 0.14
cryst syst	monoclinic	triclinic
space group	$P2_1/c$	$P\bar{1}$
a (Å)	13.872(7)	9.422(46)
b (Å)	18.790(6)	9.969(9)
c (Å)	20.971(11)	12.060(19)
α (deg)	90.00	93.08(9)
β (deg)	95.79(5)	104.89(20)
γ (deg)	90.00	102.28(17)
V (Å^3)	5438(4)	1062.5(55)
θ range for unit cell dimens (deg)	8.03−11.75	5.45−9.32
d_{calc} (g × cm^{-3})	1.462	1.511
μ (mm^{-1})	0.945	1.188
T_{min}, T_{max}	0.610, 0.282	0.847, 0.714
scan type	$\omega-2\theta$	$\omega-2\theta$
θ range (deg)	2−25	2−25
reflns measured	$-16 < h < 16$ $0 < k < 22$ $0 < l < 24$	$-11 < h < 11$ $-11 < k < 11$ $0 < l < 14$
standard reflns	3 every 400 reflns	3 every 400 reflns
tot. no. of reflns measd	9838	3921
no. of unique reflns	9556	3729
R_{int}[a]	0.1130	0.0421
R_1[b]	0.0584(5851 reflns)	0.0702(1740 reflns)
R_{all}	0.1081	0.1923
$wR2_{all}$	0.1628	0.1986
GOF[c]	1.033	0.991
no. of refined params	778	273
weighting scheme[d]	$1/[\sigma^2F_o^2 + (0.084P)^2 + 0.737P]$	$1/[\sigma^2F_o^2 + (0.0887P)^2 + 0.00P]$
$(shift/esd)_{max}$	0.001	0.000
max., min. $\Delta\rho$ (e Å^{-3})	0.50, −0.34	0.89, −0.45

[a] $R_{int} = \sum|F_o^2 - F_o^2(mean)|/\sum[F_o^2]$. [b] $R_1 = \sum||F_o| - |F_c||/\sum|F_o|$ (calculated on reflections with $I > 2\sigma_I$). [c] GOF $= S = [\sum[w(F_o^2 - F_c^2)^2]/(n-p)]^{0.5}$, where n is the number of reflections and p is the total number of parameters refined. [d] $P = [\mathrm{Max}(F_o^2,0) + 2F_c^2)/3]$.

X-ray Data Collection and Processing. Crystal data and details on the crystallographic study are reported in Table 1 (Cu(I) complexes) and Table S4 (Cu(II) complexes). Unit cell parameters and intensity data were obtained on an Enraf-Nonius CAD-4 four-circle diffractometer. All X-ray measurements were performed at room temperature using graphite-monochromated Mo Kα radiation (λ = 0.71073 Å). Calculations were performed with the WinGX software.[11] Correction for *Lp* was applied for all the crystals. Empirical absorption correction[12] was applied for all the crystals except $[Cu^{II}(\mathbf{4})](CF_3SO_3)_2$, for which no suitable reflections for a ϕ-scan were found in the range $80° < \phi < 90°$. All the structures were solved by direct-methods (SIR92)[13] and refined on F^2 by full-matrix least-squares using SHELXL-97.[14] The

(10) Gennett, T.; Milner, D. F.; Weaver, M. J. *J. Phys. Chem.* **1985**, *89*, 2787.
(11) Farrugia, L. J. WinGX-97, *An Integrated System of Publicly Available Windows Programs for the Solution, Refinement and Analysis of Single-Crystal X-Ray Diffraction*; University of Glasgow, 1997.
(12) North, A. C. T.; Philips, D. C.; Mathews, F. S. *Acta Crystallogr., Sect. A* **1968**, *24*, 351.
(13) Altomare, A.; Cascarano, G.; Giacovazzo, C.; Gualardi, A. *J. Appl. Crystallogr*. **1993**, *26*, 343−350.
(14) Sheldrick, G. M. *SHELXL-97, A Program for Crystal Structure Analysis*; Sheldrick 4M, 1998.

non-H atoms were refined anisotropically. For $[Cu^{II}(\mathbf{4})](CF_3SO_3)_2$ the H atoms were located in the difference Fourier maps and refined isotropically. In the other three structures the H atoms were inserted in the calculated positions and not refined. The asymmetric unit of the complex $[Cu^{I}(\mathbf{5})](ClO_4)_2$ includes two molecules of CH_3CN, one of which was disordered. Any attempt to refine two alternative positions for this group was unsuccessful. Atomic scattering factors were taken from *International Tables for X-ray Crystallography*.[15] Diagrams of the molecular structures were produced by the ORTEP program.[16]

Results and Discussion

(1) Structures in the Solid State. Cu^{II} Complexes. In this work, the crystal and molecular structure of the Cu^{II} complexes $[Cu^{II}(\mathbf{3})](CF_3SO_3)_2$ and $[Cu^{II}(\mathbf{4})](CF_3SO_3)_2$ have been determined by X-ray diffraction experiments. In both cases, a monomeric molecular cation was found, with a Cu^{2+} ion coordinated by the four sp^2 nitrogen atoms of a single ligand in a nearly square-planar fashion (see S5 and S6 in the Supporting Information), with two additional trifluoromethanesulfonate anions weakly bound through an oxygen atom in the apical positions of a significantly elongated octahedron, as expected on the basis of what was already found with ligand **1**. In addition, for complex $[Cu^{II}(\mathbf{3})](CF_3SO_3)_2$, the crystal structure definitely rules out any intra- or intermolecular interaction of Cu^{2+} with the thiazole sulfur atoms, which are not coordinating.

Cu^{I} Complexes. Crystal and molecular structures of Cu^{I} complexes with ligand **1**, or related complexes, have been already reported.[7b,17,18] In all cases, dimeric 2:2 metal/ligand molecular cations have been obtained. However, different conformations have been found depending on (i) the spacer connecting the two imino-heterocycle halves; (ii) the nature of the heterocycle; (iii) the counteranion. In the case of ligand **1** one nonhelical ("box-like") and two different double-helical structures have been reported,[7b] one of which is very similar to what is described for the Cu^{I} complex of a ligand strictly resembling **4**, with $-Br$ substituents instead of $-CH_3$.[17] Moreover, for a ligand resembling **5** and **6**, i.e., with a *cis*-1,2-diiminocyclohexane spacer and pyridine as the heterocycle, a double-helical dimeric structure has been reported,[18] but with a different d^{10} cation, Ag^{I}. In this work, one helical and one nonhelical ("box-like") dimeric structure have been found in the solid state. In the case of the complex $[Cu^{I}_2(\mathbf{5})_2](ClO_4)_2 \cdot 2CH_3CN$, in the $[Cu^{I}_2(\mathbf{5})_2]^{2+}$ molecular cation each Cu^{I} center is coordinated by two imino-quinoline bidentate units, each belonging to one half of two different ligands. The coordination at the copper centers is distorted tetrahedral, and the whole complex is an HT (head to tail)[19] double helix (Figure 3a).

It has to be noted that each ligand is arranged in such a way that its two imino-quinoline halves are not equivalent: half is in fact in an almost face-to-face arrangement with respect to half of the second ligand (the two quinoline heterocycles form an angle of 5.2(1)°, with C−C distances ranging from 3.239(6) to 3.510(7) Å), while the other half points away from the molecular cation and is isolated. The two ligands are related by one pseudo-C_2 axis, which allows each single ligand to superimpose on the other, but no symmetry element relates the two halves of the same ligand. Noticeably, this "unsymmetrical" arrangement with nonequivalent halves of the same ligand

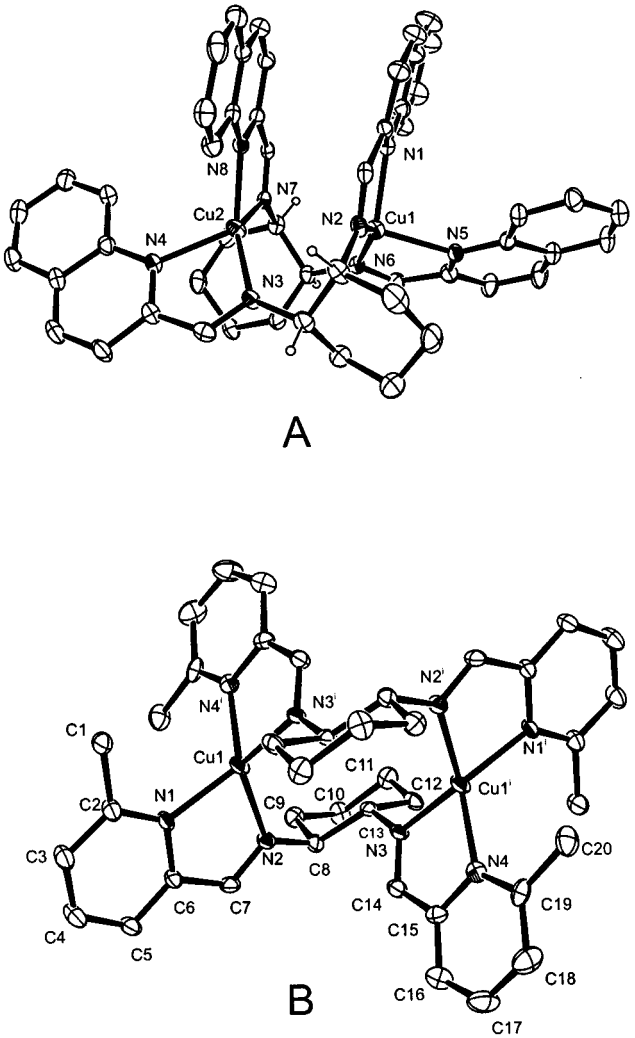

Figure 3. (a) ORTEP view of $[Cu^{I}_2(\mathbf{5})_2](ClO_4)_2 \cdot 2(CH_3CN)$ with displacement ellipsoids at 20% probability level. The hydrogen atoms, the perchlorate anions, and the acetonitrile molecules have been omitted for clarity. Only the Cu and N atoms have been labeled. Selected bond lengths: Cu1−N1 2.066(4) Å; Cu1−N2 2.053(4) Å; Cu1−N5 2.151(4) Å; Cu1−N6 2.012(4) Å; Cu2−N3 2.018(4) Å; Cu2−N4 2.111(4) Å; Cu2−N7 2.064(4) Å; Cu2−N8 2.043(4) Å. Selected bond angles: N1−Cu1−N2 81.1(1)°; N1−Cu1−N5 99.9(1)°; N1−Cu1−N6 126.4(1)°; N2−Cu1−N5 118.6(1)°; N2−Cu1−N6 145.3(1)°; N5−Cu1−N6 80.6(1)°; N3−Cu2−N4 81.2(2)°; N3−Cu2−N7 136.6(2)°; N3−Cu2−N8 128.8(1)°; N4−Cu2−N7 117.3(1)°; N4−Cu2−N8 114.8(1)°; N7−Cu2−N8 81.3(1)°. The Cu1···Cu2 distance is 3.388(2) Å. (b) ORTEP view of $[Cu^{I}_2(\mathbf{10})_2](ClO_4)_2$ with 20% probability ellipsoids. The asymmetric unit and both the Cu atoms and the N atoms of the equivalent ligand are labeled. Hydrogen atoms and perchlorate anions have been omitted for clarity. Selected bond lengths: Cu1−N1 2.023(7) Å Cu1−N2 2.005(10) Å; Cu1−$N3^{i}$ 2.034(7) Å; Cu1−$N4^{i}$ 2.036(7) Å. Selected bond angles: N1−Cu1−N2 81.5(4)°; N1−Cu1−$N3^{i}$ 128.0(3)°; N1−Cu1−$N4^{i}$ 122.7(3)°; N2−Cu1−$N3^{i}$ 123.9(3)°; N2−Cu1−$N4^{i}$ 123.8(3)°; $N3^{i}$−Cu1−$N4^{i}$ 82.8(3)°. The Cu1···Cu1^{i} distance is 4.825(11) Å. Symmetry codes: $-x, -y, -z$.

closely resembles what is already described for the Ag^{I} complex of the mentioned *cis*-cyclohexadiiminepyridine ligand[18] and for one of the Cu^{I} complexes (ClO_4^- anion) of the "trans" ligand **1**.[7b] Also the complex $[Cu^{I}_2(\mathbf{4})_2](ClO_4)_2$ contains a two-ligand, two-metal dimeric cation, $[Cu^{I}_2(\mathbf{4})_2]^{2+}$, in which the Cu^{+} cations are coordinated by two imino-pyridine halves of two different ligands. However, the $[Cu^{I}_2(\mathbf{4})_2]^{2+}$ cation is "box-like", i.e., not of helical nature (Figure 3b). It contains one *R*,*R* and one *S*,*S* isomer of ligand **4**, so it is better formulated as $[Cu^{I}(R,R\text{-}\mathbf{4})(S,S\text{-}\mathbf{4})]^{2+}$. Its structure is similar to another of the two structures

(15) *International Tables for X-ray Crystallography*; Kynoch: Birmingham, England, 1974; Vol. 4, pp 99−101 and 149−150.
(16) Farrugia, L. J. *J. Appl. Crystallogr.* **1997**, *30*, 565.
(17) Masood, M. A.; Enemark, E. J.; Stack, T. D. P. *Angew. Chem., Int. Ed.* **1998**, *37*, 928.
(18) van Stein, G. C.; van Koten, G.; Vrieze, K.; Brevard, C.; Spek, A. L. *J. Am. Chem. Soc.* **1984**, *106*, 4486.
(19) Knof, U.; von Zelewky, A. *Angew. Chem., Int. Ed.* **1999**, *38*, 302.

Table 2. λ_{max} Values (nm) for Cu^{I} (MLCT Band) and Cu^{II} (d−d Band) Complexes of Ligands **1**−**8**[a]

	1	**2**	**3**	**4**	**5**	**6**	**7**	**8**
Cu^{I}	536[a] (3500)	558 (6250)	454 (2800)	491 (3100)	543 (5400)	570 (6400)	477 (2900)	535 (6500)
Cu^{II}	668[a] (105)	700 (105)	616 (118)	698 (115)	672 (150)	716 (240)	622 (144)	677 (200)

[a] Molar extinction coefficients are in parentheses. [a] Reference 7b.

described for $[Cu^{I}_2(\mathbf{1})_2]^{2+}$ (ClO_4^- as anion),[7b] in which one *R,R* and one *S,S* ligand were again coupled in the same molecular cation: the coupling of two ligands of opposite handedness thus seems the rationale behind the formation of "box-like" instead of helical dimeric structures (see also ref 17 for the helical complexes of an enantiomerically pure ligand resembling **4**). Finally, it has to be noted that also in the case of $[Cu^{I}(R,R\text{-}\mathbf{4})(S,S\text{-}\mathbf{4})]^{2+}$, while the two ligands are equivalent (they are related by an inversion center), the two halves of the same ligand are not equivalent.

(2) Structures and Properties in Solution. **Cu(II) Complexes**. All the Cu(II) complexes reported in this work are momomeric and of distorted square-planar geometry, as predictable on the basis of the ligands' geometry and as confirmed by X-ray and mass and UV−vis spectroscopy. In particular, wavelengths and extinction coefficients of the bands found in the UV (CT) and visible range (d−d), which are collected in Table 2, are consistent with what is already reported for distorted square-planar Cu(II) complexes with tetradentate ligands featuring sp^2 nitrogen donors.[7d,20]

The value of λ_{max} for the d−d band of Cu^{II} complexes with ligands **1**−**8** is connected to the nature of the ligand−metal in-plane interactions. Table 2 shows that, among the ligands having the same spacer between the imino-heterocycle halves, λ_{max} shifts toward longer wavelengths on increasing the size of the heterocyclic fragment. This can be reasonably associated with the decreased hardness of the N-donor on increasing the heterocycle delocalization. The complex with ligand **4**, however, even if featuring the same *trans*-1,2-cyclohexanediyl spacer and a methylpyridine heterocycle, displays a d−d band with a very high λ_{max} value, 698 nm. This gives account of the serious distortion imposed on the ideal square-planar coordination by the two bulky methyl groups (see also Figure S6). Moreover, it is interesting to note that less pronounced variations of the λ_{max} values are instead observed on keeping the heterocylcle constant and on varying the nature of the spacer, e.g., in the series of complexes with ligands **1**, **5**, and **8**, which feature quinoline heterocycles and *trans*-1,2-cyclohexanediyl, *cis*-1,2-cyclohexanediyl, and 1,2-ethanediyl spacers, respectively, thus indicating that these ligands are capable of wrapping around the Cu^{II} cation with comparable geometries. Finally, the d−d band of the Cu^{II} complexes with ligands **1**−**8** (and in some cases also the CT bands found in the UV zone) has been also used to check the stability of their acetonitrile solutions: the variation of the absorbance of the d−d band was checked every 1 h for a 2-day period on freshly prepared solutions of the chosen solid complex. Absorbance variations of less than 2% were observed in any case, except with $[Cu^{II}(\mathbf{2})](CF_3SO_3)_2$, if the solutions were kept under nitrogen. In the case of the complex of ligand **2**, spontaneous reduction to a Cu^{I} complex was disclosed (with the onset of the corresponding band at 558 nm), which reached ∼15% after 2 days. When the solutions were exposed to air, the behavior of the complexes with ligands **1**−**6** was found to be the same as under an inert atmosphere. A moderate tendency to hydrolysis was instead observed for the Cu^{II} complexes of **7** and **8**, for which decomposition of 2−5% of the starting material was found after 2 days.

Cu(I) Complexes. A 2:2 stoichiometry holds for all the Cu(I) compounds described in this work, as demonstrated by coupling UV/vis titrations with mass (ESI) spectra results: on titrating acetonitrile solutions of the chosen ligand with substoichiomeric quantities of Cu^{I} from an acetonitrile solution of $[Cu^{I}(CH_3CN)_4]ClO_4$, spectral changes end at a metal/ligand molar ratio of 2:2. Sharp isosbestic points and the intense MLCT band, typical of Cu^{I} complexes with sp^2 nitrogen donors belonging to an extended π-system, are always observed (see Table 2 for λ_{max} and extinction coefficients). Mass spectra, carried out with ESI technique on acetonitrile solutions containing Cu^{I} and the chosen ligand in a 2:2 molar ratio or prepared from solid samples of the chosen Cu^{I} complex, display the peak required for $\{[Cu^{I}_2(\mathbf{L})_2](ClO_4)\}^+$ species, ensuring that the stoichiometry observed by spectrophotometric titration experiments is authentically 2:2 and not 1:1. However, as also suggested by the variety of dimeric isomers found in the solid state for the molecular cation $[Cu^{I}_2(\mathbf{1})_2]^{2+}$,[7b] care must be taken in evaluating which dimeric form is present in solution. For almost all the Cu(I) complexes prepared and studied in this work, the ^1H NMR spectra in the aromatic region, i.e., the signals relative to the heterocyclic and imine protons, help determine which structure holds in solution (full spectral details are reported in S3). The ^1H NMR spectra of the Cu(I) complexes of the ligands containing the 1,2-*trans*-cyclohexanediyl spacer can be examined together (excluding that containing the thiazole-functionalized ligand **3**, vide infra). The spectrum of the complex cation $[Cu^{I}_2(\mathbf{2})_2]^{2+}$ was obtained in CD_3CN, by dissolution of solid samples of its perchlorate salt. Only one set of signals is observed in the aromatic zone, displaying the same number and multiplicity of the signals of the free ligand, indicating that only a homochiral symmetrical helical dimer is present (heterochiral "box-like" dimers or unsymmetrycal homochiral helicates would give rise to aromatic and imine signals split into two subsets[7b,21]). An analogous situation is found for the CD_3CN solutions obtained from the same crystalline samples of $[Cu^{I}_2(\mathbf{4})_2](ClO_4)_2$ which were used for crystal structure determination. The spectrum contains only one set of signals, as in the free ligand: the two halves of each **4** ligand are equivalent, and the two **4** ligands assembled in $[Cu^{I}_2(\mathbf{4})_2]^{2+}$ are also equivalent between them. This situation is again compatible only with a homochiral symmetrical double-helical structure for the $[Cu^{I}_2(\mathbf{4})_2]^{2+}$ cation in solution, and this implies a serious rearrangement with respect to what is found in the solid (a heterochiral, unsymmetrical molecular cation, vide supra), which takes place in the few seconds occurring between dissolution and measurement. However this is not surprising, as it has already been demonstrated that either bulky heterocycles or bulky substituents on the heterocycles appended to the *trans*-1,2-cyclohexanediyl spacer strongly favor the formation in solution of homochiral helical complexes with Cu^{I}.[17,21] Moreover, it has been shown that very fast rearrangements take place in the complexes of Cu^{I} and Cu^{II} with ligands **1**−**8** (vide

(20) Lehn, J.-M.; Sauvage, J.-P.; Simon, J.; Ziessel, R.; Piccinni-Leopardi, C.; Declercq, J.-P.; Van Meerssche, M. *Nouv. J. Chim* **1983**, *7*, 413.

(21) Amendola, V.; Fabbrizzi, L.; Mangano, C.; Pallavicini, P.; Roboli, E.; Zema, M. *Inorg. Chem.* **2000**, *39*, 5803.

infra and ref 7b). As a final remark on the *trans*-1,2-cyclohexanediyl-containing complexes, not much can be said on the solution structure of the Cu(I) dimeric complex with the thiazole-functionalized ligand **3**. Solutions of $[Cu^{I}_2(\mathbf{3})_2]^{2+}$ were prepared in CD_3CN from solid samples of its perchlorate salt. The obtained ^1H NMR spectra showed the same number of signals as for the free ligand, but the observed peaks were very broad and not structured. This was probably due to the oxidation of some Cu^{I} to Cu^{II} species, which could not be prevented under the employed experimental conditions and which was confirmed by mass (ESI) spectra, which also showed trace signals for the $[Cu^{II}(\mathbf{3})]^{2+}$ cation. Also the ^1H NMR spectra of the two Cu^{I} complexes of the ligands containing the *cis*-1,2-cyclohexanediyl spacer can be examined together. By dissolving crystals of $[Cu^{I}_2(\mathbf{5})_2](ClO_4)_2$ in CD_3CN an NMR spectrum was obtained that featured heterocycle and imine proton signals split into two twin sets, indicating that in acetonitrile the HT unsymmetric helical structure found in the solid state is maintained. The same NMR splitting was observed for CD_3CN solutions of the complex $[Cu^{I}_2(\mathbf{6})_2](ClO_4)_2$ (Figure S7), so that an HT unsymmetric helical structure can be assigned also to its molecular cation $[Cu^{I}_2(\mathbf{6})_2]^{2+}$, strongly suggesting that the *cis*-1,2-cyclohexanediyl spacer leads only to this kind of helical structure, independent of the bulkiness of the appended heterocycle (as confirmed also by analogous results for Ag(I)[18] complexes of a related ligand). Finally, the ^1H NMR spectra in CD_3CN of compounds $[Cu^{I}_2(\mathbf{7})_2](ClO_4)_2$ and $[Cu^{I}_2(\mathbf{8})_2](ClO_4)_2$ must be considered. The two spectra display similar features as, in both cases, besides a change in the chemical shift of the aromatic and imine protons with respect to the corresponding free ligand, the number and multiplicity of these signals remain the same as found for uncomplexed **7** and **8** ligands. This indicates that a symmetrical configuration must exist in solution for $[Cu^{I}_2(\mathbf{7})_2]^{2+}$ and $[Cu^{I}_2(\mathbf{8})_2]^{2+}$, whose helical nature can be made clear by observing the signals of the $-CH_2-CH_2-$ bridge protons (Figure S8): in the free ligands, the $-CH_2-CH_2-$ signals appear of course as a four-proton singlet, but in the two complexes they split into an AB pattern, indicating that ligands lose their symmetry by adopting a helical disposition, as already well established for complexes of comparable nature.[22,23]

As regards the UV/vis spectra in acetonitrile of the Cu^{I} complexes of the **L** ligands (**L** = **1**−**8**), remarkably different values are found for the λ_{max} of the intense MLCT visible transition (see Table 2). In particular, for complexes with ligands containing the same spacer between the heterocylces, the value shifts toward lower energy values on increasing the delocalization of the extended imino-heterocycle system. On the other hand, only slight variations were instead observed in the series of complexes of Cu^{I} with ligands featuring a different spacer and the same heterocycle. Finally, UV/vis spectra were taken at time intervals of 1 h for 2 days on acetonitrile solutions of pure solid samples of the complexes between Cu^{I} and ligands **1**−**8**, to check their stability toward air and moisture. In particular, the intense visible MLCT band is a sensitive probe for oxidation and hydrolysis. Negligible variations (less than 2% decrease) were observed for the complexes of ligands **1**, **2**, **4**, **5**, **6**, and **8**. Only in the case of the complexes of **3** and **7** was a decrease of 15% and 3% of the MLCT band (and thus of the Cu^{I} complex concentration) observed over a 2-day period, depending on the experimental conditions.

(22) (a) Lehn, J.-M.; Rigault, A. *Angew. Chem., Int. Ed.* **1988**, *27*, 1095. (b) Youinou, M.-T.; Ziessel, R.; Lehn, J.-M. *Inorg. Chem.* **1991**, *30*, 2144.
(23) Bilyk, A.; Harding, M. M. *J. Chem. Soc., Dalton Trans.* **1994**, 77.

Table 3. Oxidation Potentials, Reduction Potentials, and ΔE Values ($\Delta E = E_{ox} - E_{red}$) for Cu^{I} Complexes of the Indicated Ligands (Cu^{II} Complexes Gave Identical Results)[a]

	1[b]	**2**	**3**	**4**	**5**	**6**	**7**	**8**
E_{ox}	615	530	395	385	430	723	338	692
E_{red}	−20	20	−101	−106	−250	−241	−397	−10
ΔE	635	510	496	491	680	964	732	702

[a] E values are referred to the Fc^+/Fc couple. All values were measured in acetonitrile, 0.1 M in $(but)_4NClO_4$, with cyclic voltammetry technique, at a scan rate of 200 mV/s. [b] Reference 7b.

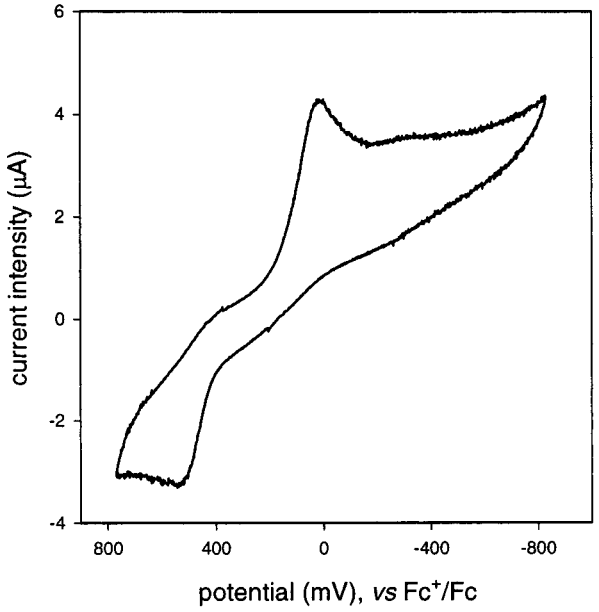

Figure 4. Cyclic voltammetry profile for $[Cu^{I}_2(\mathbf{2})_2](ClO_4)_2$, in CH_3CN. Potential was scanned between +800 and −800 mV, starting at 300 mV. The second cycle, which features both oxidation and reduction waves, is reported.

(3) Electrochemistry: Assembling/Disassembling Processes and Hysteresis. Solid-state isolation and UV/vis band duration results have demonstrated that the complexes between ligands **1**−**8** and Cu^{I}/Cu^{II} are bistable, both as solid samples, and the corresponding acetonitrile solutions of Cu^{I} and Cu^{II} complexes are fairly stable under the same conditions. The examination of their electrochemical properties in acetonitrile stresses how each copper/ligand system can be made to electrochemically change between its two states and to display hysteresis in this process. Cyclic voltammetry experiments were performed on acetonitrile solutions of the $[Cu^{I}_2(\mathbf{L})_2](ClO_4)_2$ and $[Cu^{II}(\mathbf{L})](CF_3SO_3)_2$ complexes (**L** = **1**−**8**). In all cases, almost superimposable profiles were found for the cupric and cuprous complexes of the same ligand, and very similar profiles, as regards shape and number of signals, were disclosed for all complexes. In particular, the voltammetric profiles display a reduction wave centered at E_{red} potential, which appears to be completely irreversible (i.e., it lacks its corresponding return wave), while a separate, irreversible oxidation (again without its corresponding reduction wave) is found at potential E_{ox}, with the $\Delta E = E_{ox} - E_{red}$ difference ranging from ∼500 to ∼1000 mV. E_{ox}, E_{red}, and ΔE values for all the examined complexes are summarized in Table 3. As an example, the voltammetric profile for $[Cu^{I}_2(\mathbf{2})_2](ClO_4)_2$ is illustrated in Figure 4.

On dissolving a $[Cu^{I}_2(\mathbf{2})_2](ClO_4)_2$ sample in acetonitrile and starting the voltammetric experiment at + 300 mV vs Fc/Fc^+ ($+800 > E > -800$ mV vs Fc^+/Fc), on going toward negative potentials, no reduction wave is found for the first cycle, while,

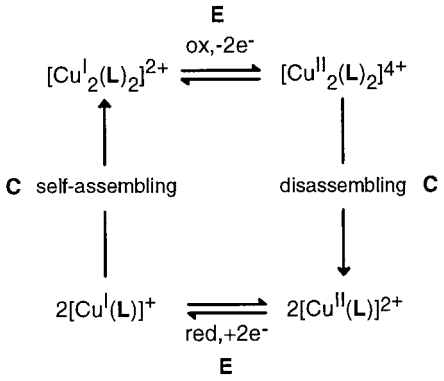

Figure 5. Electrochemical "square scheme" for the transformation of systems $[Cu^{I}_2(\mathbf{L})_2]^{2+}$ into $[Cu^{II}(\mathbf{L})]^{2+}$ ($\mathbf{L} = \mathbf{1}-\mathbf{8}$): horizontal events are of electrochemical (E) nature, vertical events are of chemical (C) nature.

on reverting the scanning direction, a two-electron oxidation peak appears at $E_{ox} = +530$ mV vs Fc^+/Fc. No return wave for this peak is found, while, on scanning again toward negative potentials, a one-electron reduction wave appears now at $E_{red} = +20$ mV vs Fc^+/Fc, which also has no return wave. It has to be noticed that no return wave is found both for oxidation and reduction even at the maximum scan rate allowed by the instrumentation available to us (20 V/s). Irreversibility originates from the fast disassembling process $[Cu^{II}_2(\mathbf{2})_2]^{4+} \rightarrow 2[Cu^{II}(\mathbf{2})]^{2+}$ taking place after oxidation of the Cu^I helicate and from the fast self-assembling process $2[Cu^{I}(\mathbf{2})]^{+} \rightarrow [Cu^{I}_2(\mathbf{2})_2]^{2+}$ following the reduction of the Cu^{II} complex. The behavior of the system can thus be summarized with a "square scheme"[24] (Figure 5), which is made by combination of two EC processes.

Both for square schemes[25] and for simple EC processes[26] theories have been developed that allow the determination of the kinetic constants for the chemical reaction following the electrochemical event.[27] However, regarding this, the determination of the authentic $E_{1/2}$ potentials of the separate $[Cu^{I}_2(\mathbf{L})_2]^{2+} = [Cu^{II}_2(\mathbf{L})_2]^{4+} + 2e^-$ and $[Cu^{II}(\mathbf{L})]^{2+} + e^- = [Cu^{I}(\mathbf{L})]^{+}$ redox events ($\mathbf{L} = \mathbf{1}-\mathbf{8}$) is crucial,[26] and to evaluate them, it is necessary to perform CV experiments at such a high scan rate that a return wave appears in the voltammetric profile. Unfortunately, in our case, for all complexes no trace of return wave appears even at the fastest scan rate allowed by our experimental apparatus, so that neither $E_{1/2}$ for the two redox events nor, consequently, any kinetic constant can be determined. However, by considering that in the time needed to scan the potential at 20 V/s from 100 mV higher than E_{red} to 100 mV lower than it, and return, no trace of oxidation wave appears, it can be stated that the transient species $[Cu^{I}(\mathbf{L})]^{+}$ has a lifetime less than 20 ms, during which time it fully self-assembles to $[Cu^{I}_2(\mathbf{L})_2]^{2+}$ (similar consideration can be made for the oxidation + disassembling process). It has to be stressed that only the single oxidation or reduction electrochemical processes are to be considered irreversible, as they are followed by a fast chemical reaction (with the species at equilibrium and with the equilibrium completely displaced to the right). On the other hand, it appears that both the assembling/disassembling and the electrochemical

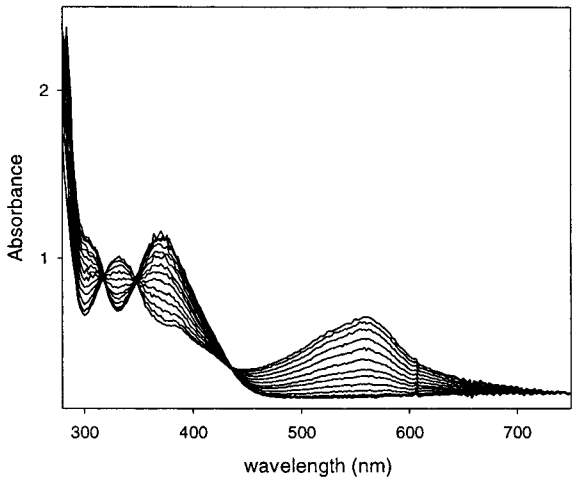

Figure 6. UV/vis spectra taken during the transformation, in a CPC experiment, of $[Cu^{I}_2(\mathbf{2})_2]^{2+}$ into $[Cu^{II}(\mathbf{2})]^{2+}$. The band at 558 nm decreased in intensity, while the band at 370 nm increased. An identical series of spectra, but in the reverse order, was obtained during the CPC reduction of $[Cu^{II}(\mathbf{2})]^{2+}$ into $[Cu^{I}_2(\mathbf{2})_2]^{2+}$. Due to the low concentration, the weak d−d band of the Cu^{II} complex at 680 nm cannot be observed.

processes leave the participating species intact, that is, no decomposition is observed. Thus, the electrochemically driven assembling/disassembling overall process, i.e., the transformation $[Cu^{I}_2(\mathbf{L})_2]^{2+} = 2[Cu^{II}(\mathbf{L})]^{2+} + 2e^-$, is to be considered as perfectly reversible. This is confirmed by controlled potential coulometry (CPC) experiments, in which the electrochemically induced transformations taking place in solution have been moniterd by UV/vis spectroscopy. Also in these experiments, similar results have been obtained for the complexes of all ligands. The case of the complexes of the phenanthridine-containing ligand **2** is reported in Figure 6 as an example. During a CPC experiment, in a deep violet solution of $[Cu^{I}_2(\mathbf{2})_2](ClO_4)_2$ current passage was observed when the applied potential was raised 50 mV over the E_{ox} value. The MLCT band of the Cu^I complex at 558 nm decreased, while the high-energy CT band of the Cu^{II} complex, at 370 nm increased, and three sharp isosbestic points were also found.

After the passage of 2 mol of electrons per mol of $[Cu^{I}_2(\mathbf{2})_2]^{2+}$ the current passage stopped and no more variations were observed in the spectrum, which was found to be superimposable on that of an authentic sample of $[Cu^{II}(\mathbf{2})](CF_3SO_3)_2$, indicating that the [oxidation+diassembling] process was complete. The solution changed to the pale green color typical of the dilute solutions of the Cu^{II} complex of ligand **2**. When the applied potential was lowered to 100 mV under the E_{red} value, current passage was observed again and the same series of spectra displayed in Figure 6 was recorded, but in the reverse order. After the passage of 1 mol of electrons per mol of complex the current stopped, and spectra superimposable on the spectrum of the starting $[Cu^{I}_2(\mathbf{2})_2](ClO_4)_2$ solution were found, indicating that the [reduction+self-assembling] process was complete. Finally, it has to be noticed that the cycle has been repeated 15 times without significant variations in the final spectra.

According to the results reported so far in this paper, under the variation of the applied potential solutions of copper (oxidation state I or II) complexes of ligands $\mathbf{1}-\mathbf{8}$ display hysteresis. This is summarized in Figure 1b, which sketches a hysteresis scheme adapted to our systems: the parameter made to vary is now the applied potential, E, and the two states between which the system changes (S_1 and S_2 in Figure 1a) are $[Cu^{I}_2(\mathbf{L})_2]^{2+}$ and $[Cu^{II}(\mathbf{L})]^{2+}$. As a matter of fact, solutions

(24) Jacq, J. *J. Electroanal. Chem.* **1971**, *29*, 149.
(25) Vallat, A.; Person, L.; Roullier, L.; Laviron, E. *Inorg. Chem.* **1987**, *26*, 332.
(26) (a) Evans, D. H. *Chem. Rev.* **1990**, *90*, 739. (b) Bard, A. J.; Faulkner, L. R. *Electrochemical Methods*; Wiley: New York, 1980.
(27) The measured ΔE values undergo a contraction of 40−60 mV every 10-fold decrease of the scan rate, as expected (ref 26b) for the coupling of one EC involving a two-electron redox change with an EC involving a one-electron change.

containing one of the eight possible $[Cu^{I}_2(\mathbf{L})_2]^{2+}$ complexes remain unchanged (state 1), if the applied potential is raised, but mantained under E_{ox} (noticeably, even if the potential is made to vary in the opposite direction and goes below E_{red}, no change is observed[28]). When E is raised to values $\geq E_{ox}$, oxidation and disassembling are observed, so that the system goes straight to its second state, $[Cu^{II}(\mathbf{L})]^{2+}$. In this state, E can be lowered without changes if it is mantained over E_{red} (again, further raising of the potential higher than E_{ox} up to the solvent discharge limit results in no change). When E is lowered to values $\leq E_{red}$, reduction and self-assembling are observed, so that the system switches back to $[Cu^{I}_2(\mathbf{L})_2]^{2+}$. Thus, in the interval $E_{red}-E_{ox}$ the system can exist either as $[Cu^{I}_2(\mathbf{L})_2]^{2+}$ or $[Cu^{II}(\mathbf{L})]^{2+}$ depending on its electrochemical history. Moreover, the electrochemical hysteresis scheme displays a "sense of rotation", as the monomeric Cu^{II} form of course does not transform into the dimeric Cu^{I} form on increasing E over E_{ox} and, vice versa, the Cu^{I} helical dimer cannot be switched back to the Cu^{II} complex on lowering E below E_{red}. Besides displaying a hysteresis profile, solutions of the $\mathbf{L}/Cu^{I}/Cu^{II}$ systems have intrinsic properties that allow information storage: the $[Cu^{I}_2(\mathbf{L})_2]^{2+}$ helical dimers feature an intense MLCT band ($\epsilon = 10^3-10^4$) in the 450−570 nm range, while, in the same wavelength range, the corresponding Cu^{II} monomers do not absorb. Hence, in a colorless solution containing $[Cu^{II}(\mathbf{L})]^{2+}$, an information can be written by lowering the potential below E_{red}: $[Cu^{I}_2(\mathbf{L})_2]^{2+}$ is obtained, which displays an intense band and represents a bit value of 1. This bit value is maintained either if no potential is applied to the solution (i.e., it is a permanent information) or if any potential $< E_{ox}$ is applied. On the other hand, when a potential $\geq E_{ox}$ is applied, the information is erased: the Cu^{I} helical dimer is transformed in the Cu^{II} monomer, which has no bands in the 450−600 wavelength interval and thus represents a bit value of 0. Quite interestingly, with these systems the portion of solution capable of working as a memory can be scaled down, at least in principle, to such a small volume to contain only a single $[Cu^{I}_2(\mathbf{L})_2]^{2+}$ molecule, so that also in this case, it is possible to think of $[Cu^{I}_2(\mathbf{L})_2]^{2+}$ as a "single-molecule memory".

As a final remark, as shown in Table 3 the E_{ox}, E_{red}, and ΔE values for copper complexes of the **1**−**8** series are distributed over a considerably large range, as a function of the nature of the heterocycle and of the spacer in the ligand, leading to envisage the possibility of controlling at will the potential values at which, in the hysteresis loop, transitions between the two states take place. As already mentioned, the observed E_{red} and E_{ox} values are not coincident with the $E_{1/2}$ values of the corresponding redox reaction. For EC reactions, the authentic $E_{1/2}$ values differ from the observed E_{ox} and E_{red} by a value that depends on the scan rate and on the kinetic constant of the chemical reaction following the redox event.[26] However, assuming that the kinetics of the $2[Cu^{I}(\mathbf{2})]^{+} \rightarrow [Cu^{I}_2(\mathbf{2})_2]^{2+}$ self-assembling process (or of the $[Cu^{II}_2(\mathbf{2})_2]^{4+} \rightarrow 2[Cu^{II}(\mathbf{2})]^{2+}$ disassembling process) are not too different for the series of complexes with ligands **1**−**8**, comparisons can be done on the values reported in Table 3, which have been obtained using a 200 mV/s scan rate in all cases. The assumption is reasonable if one considers that for a fast chemical reaction following an n-electron redox event a $30/n$ mV shift of the peak potential of the observed irreversible signal is expected for a 10-fold increase of the kinetic constant.[26b] As a rule of thumb, in the series of complexes with ligands **1**−**4**, which feature the *trans*-1,2-cyclohexanediyl spacer between the imino-heterocycle halves, on increasing the dimensions of the heterocycle, and thus the softness of the N-donors, the reduction process becomes easier and easier. This is associated with the increased donor softness, which stabilizes the Cu^{I} state and destabilizes the starting Cu^{II} state, by lowering the crystal field stabilization energy, as also indicated by the trend in the d−d band maxima. The same is observed when moving from the pyridine-functionalized ligand **7** to the quinoline-functionalized ligand **8**, which feature the same 1,2-ethanediyl spacer, and, although to a lesser extent, for the **5** and **6** couple, which feature the *cis*-1,2-cyclohexanediyl spacer. As regards the oxidation potentials, the trend is clear only on passing from complexes of ligands with small heterocycles (**3**, **4**, and **7**) to those with ligands containing quinoline or phenanthridine. A significant increase of the E_{ox} value is observed as, most probably, the donor properties effect prevails: N atoms belonging to small heterocycles display more favorable interactions with Cu^{II} than with Cu^{I}, in comparison to ligands with extended heterocycles. On the other hand, by comparing the complexes of ligands featuring quinoline heterocycles (**1** and **5**) with those of ligands featuring phenanthridine (**2** and **6**), different trends are found: in this case, due to the increased bulkiness of the ligands, also less predictable geometric effects should be taken into account.

(4) Concluding Remarks and Perspectives. Copper complexes of ligands **1**−**8** have been demonstrated to undergo electrochemical processes that have the features of a hysteresis cycle. The potentials at which the transition from one state to the other takes place are a function of simple parameters such as the geometry of the diimino spacer and the number of condensed rings of the appended nitrogen heterocycle. Moreover, also the λ_{max} of the MLCT band in the Cu(I) complexes is a function of the latter factor. A set of compounds is thus available that, at least in principle, could behave as molecular memories: among this set (or in its synthetically straightforward extensions) the potentials at which an information can be written and erased and the wavelength at which it could be read can be chosen over a large range of values. According to this, it could be possible, at least in principle, to prepare solutions containing two different copper/ligand complex species and to switch at will to the Cu^{I} state only one or two of them. Vice versa, having both systems at the Cu^{I} state, it would be possible to oxidize at will (and to erase the information) only one or two of them. Moreover, it has to be stressed that the two information bits stored in the two complexes coexisting in solution can be different, provided that their MLCT absorption bands are centered at significantly different wavelengths. This opens the perspective of using the systems described in this work for storing more than one information bit in the same portion of matter.[29] However, although ligands of the **1**−**8** set, or similar, display enhanced self-recognition properties when assembling on Cu(I),[17,21] a fast scrambling of the heterocycles in Cu(I) complexes coexisting in the same solution prevents the use of two complexes of the set **1**−**8** for this aim.[30] Work is now in progress in order to find other ligands not featuring the imine

(28) Going down with the potential until the solvent discharge limit, reductive stripping processes are indeed observed in some cases.

(29) Potember, R. S.; Poheler, T. O.; Hoffman, R. C.; Speck, K. R.; Benson, R. C. In *Molecular Electronic Devices II*; Carter, F. L., Ed.; Marcel Dekker: New York, 1987.

(30) ^{1}H NMR and mass (ESI) measurements strongly suggest that the observed process is not a simple ligand scrambling of the $[Cu^{I}_2(\mathbf{L1})_2]^{2+} + [Cu^{I}(\mathbf{L2})_2]^{2+} = 2[Cu^{I}(\mathbf{L1})(\mathbf{L2})]^{2+}$ type, but it involves the formation of ligands that contain both heterocycles. Although we are not able to propose a detailed mechanism, the lability of the imine moiety can be taken into consideration, especially in the presence of trace quantities of water (see: Clark, B. P.; Harris, J. R.; Timms, G. H. *Tetrahedron Lett.* **1995**, *36*, 3889).

moiety but capable of giving a similar electrochemical hysteresis behavior, due to self-assembling/disassembling processes taking place on changing the oxidation state of the coordinated copper cation. Coupling these systems with those described in this work could allow the storing of multiple information in solution.

Acknowledgment. This work was financed by Murst (Progetti di Ricerca di Interesse Nazionale).

Supporting Information Available: Listings of final atomic coordinates, anisotropic thermal parameters, all bond lengths and angles, intermolecular contacts, least-squares planes, and unit cell and packing diagrams are available as CIF files for the four crystal and molecular structures presented in this work. Tables containing ligand, Cu^{I} and Cu^{II} complex characterization data (IR, NMR, CHN analysis, and yields) and a table with the crystal and refinement data for the two Cu^{II} complexes are available. Sketches of the Cu^{II} molecular structures and representative Cu^{I} complexes' ^{1}H NMR in CD_3CN are also available. This material is available free of charge via the Internet at http://pubs.acs.org.

IC001155A